Off-Time Control of *LLC* Resonant Half-Bridge Converter to Prevent Audible Noise Generation Under a Light-Load Condition

Ho-Young Yoon, Hyeon-Seok Lee, Seok-Hyeong Ham, Hyung-Jin Choe, and Bongkoo Kang, *Member, IEEE*

***Abstract*—This paper presents a control method that can prevent audible noise generation in an *LLC* resonant half-bridge dc–dc converter under a light-load condition, while achieving the same input voltage range and power-conversion efficiency η_e as the burst-control method that generates an audible noise. The proposed method reduces switching and conduction losses at light load by skipping several pairs of switch-control pulses, while varying the switching frequency less than the normal-control method does. This skip-control method enables the *LLC* resonant converter to have a large magnetizing inductance, and to have high η_e over a wide range of load variation. At an input voltage of 385 V, an output voltage of 24 V, and a resonant frequency of 180 kHz, the proposed method achieved $\eta_e \geq 85.46\%$ for an output power range of 7.2–360 W; the highest η_e was 96.08% at $P_o = 336$ W.**

***Index Terms*—DC–DC power conversion, digital control, on–off control, pulse-frequency modulation, pulse width modulated power converters, resonant power conversion.**

I. Introduction

THE *LLC* resonant half-bridge converter [see Fig. 1(a)] is used widely for applications that require high power-conversion efficiency η_e at a heavy load (high output power) [1]–[10]. This converter operates at a fixed switching duty and generates voltage pulses by turning ON the switches SW_1 and SW_2 alternately. The resonant circuit, composed of C_r, L_r, and L_m and the $n:1$ ideal transformer, produces zero-voltage-switching conditions for the switches, and it works as a bandpass filter. The *LLC* half-bridge converter has an equivalent circuit [see Fig. 1(b)] for the fundamental component of the input pulses. The magnetizing inductor L_m of the transformer is bypassed by the load when it is heavy, so the inductor L_r resonates with the capacitor C_r with a resonance frequency $f_r = 1/(2\pi\sqrt{L_r C_r})$. In this case, the voltage conversion ratio (gain) of the converter can be varied by changing f_s (see Fig. 2). However, under a light-load condition, L_m shifts the resonance frequency to $f_{r,Q}$ and increases the gain in the inductive region ($f_s > f_{r,Q}$); as a result, f_s must be increased at a given gain. The switching loss increases as f_s increases although the switches operate under a soft-switching condition, and this increase causes a decrease in η_e when the load is light [11]–[16].

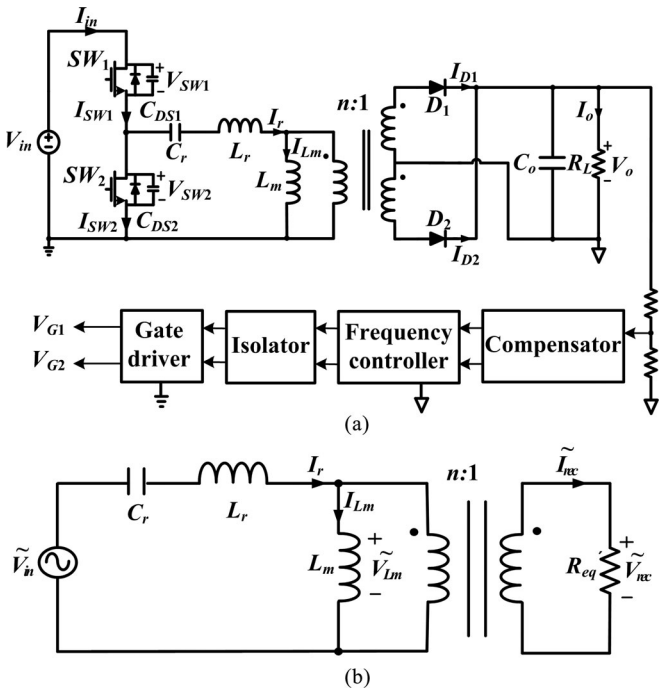

Fig. 1. *LLC* resonant half-bridge converter: (a) circuit structure and (b) equivalent circuit.

Switching loss in *LLC* resonant half-bridge converters can be reduced by using an auxiliary circuit [17], [18] or by using gate-pulse modulation [19], [20]. The auxiliary circuit changes f_r to accommodate the converter for load variation, instead of varying f_s. The switch control capacitor (SCC) in [17] consists of a capacitor connected in parallel with a bilateral switch. This SCC is connected in series with C_r, so the effective impedance Z_{eff} of the *LLC* resonant circuit can be adjusted by changing the ON duty of the bilateral switch. However, the *LLC* resonant circuit requires a gate driver for the bilateral switch, armed with

Manuscript received July 12, 2017; revised September 30, 2017; accepted November 6, 2017. Date of publication November 17, 2017; date of current version July 15, 2018. This work was supported by LG Display Co. and the Ministry of Science, ICT and Future Planning, South Korea, under the "ICT Consilience Creative Program" (IITP-R0346-16-1007) supervised by the Institute for Information & Communications Technology Promotion (IITP). Recommended for publication by Associate Editor D.G. Lamar. *(Corresponding author: Bongkoo Kang.)*

H.-Y. Yoon, H.-S. Lee, S.-H. Ham, and B. Kang are with the Department of Electrical Engineering, Pohang University of Science and Technology, Pohang 37673, South Korea (e-mail: hyyoon@postech.ac.kr; hsasdf@postech.ac.kr; ham1234@postech.ac.kr; bkkang@postech.ac.kr).

H.-J. Choe is with the LG Display Co., Ltd., Paju 10845, South Korea (e-mail: hjchoe82@lgdisplay.com).

Color versions of one or more of the figures in this paper are available online at http://ieeexplore.ieee.org.

Digital Object Identifier 10.1109/TPEL.2017.2774840

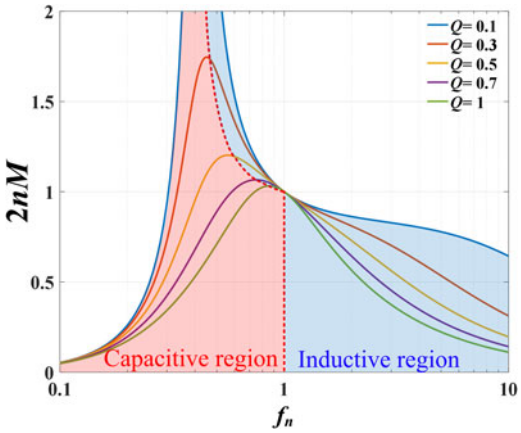

Fig. 2. $2nM$ versus f_n for the *LLC* half-bridge resonant converter for $0.1 \leq Q \leq 1$.

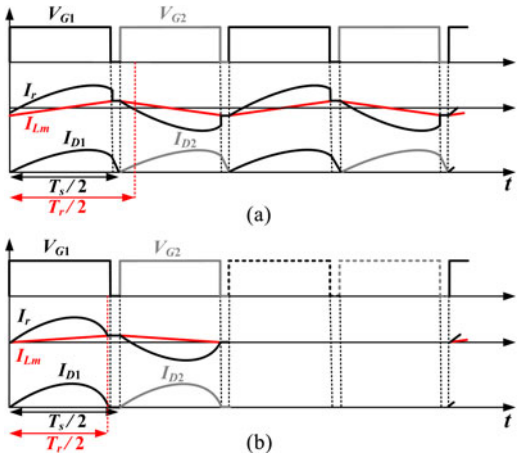

Fig. 3. Waveforms of the gate control voltages V_{G1} and V_{G2}, resonant current i_r, and rectifier input currents i_{D1} and i_{D2}: (a) for normal control and (b) for skip control.

a complicated control algorithm. The auxiliary circuit presented in [18] is connected in parallel with C_r. This circuit consists of two switches and one ripple-control inductor, and controls the ripple voltage of C_r by using the ripple-control inductor. When the converter is optimized to operate at a light load and operates at a given f_s in the capacitive region $(f_s < f_{r,Q})$, η_e under a heavy-load condition can be increased by increasing the ripple voltage of C_r, i.e., by injecting additional charge to C_r through the ripple-control inductor, that decreases Z_{eff} of the *LLC* resonant circuit. However, the additional loss in the auxiliary circuit limits further improvement of η_e under heavy load.

Z_{eff} of the *LLC* resonant circuit can also be varied using a gate-pulse modulation, without using additional components. The burst-control method proposed in [19] modulates gate-control pulses when the load is light; it turns off gate pulses periodically, which decreases the effective switching frequency $f_{s,\text{eff}}$. The power conversion occurs only when the gate signals are turned on, so the switching and conduction losses under a light-load condition are reduced. However, an audible noise is generated when the lowest component of switching frequency $f_{s,\text{lowest}}$ moves down to the audio frequency band (<20 kHz), and the output voltage ripple increases when the turn-off period increases.

A method to control the switching duty has been proposed in [20]. This method controls the voltage gain when the load is light by varying the switching duty, instead of modulating f_s; the fundamental component of input is changed by varying the switching duty although f_s is fixed at f_r. However, this method cannot be used either when the load is very light or when the input voltage V_{in} is high, because the available range of the switching duty is limited.

A method of increasing η_e and decreasing the output voltage ripple ΔV_o of the buck converter has been proposed [21]; the buck converter operates at a given f_s, regulates the voltage gain by adjusting the switching duty, but its switch subjects to a hard switching, so the converter had $\eta_e < 90\%$. This method uses two sets of numbers: N_1 and N_2 for numbers of skipped switching periods, and n_1 and n_2 for the numbers of repetition of these two different skipping periods. A combination of these four numbers gives an effective skip number $N_s = (n_1 N_1 + n_2 N_2)/(n_1 + n_2)$. The switching power loss under a light-load condition is reduced by varying N_s. However, as given in [21, Table III], N_s can increase as high as 24.5 at $I_o = 10$ mA. Then, $f_{s,\text{lowest}} = 200/(1 + 24.5) = 7.8$ kHz, which belongs to the audible frequency range. One could increase f_s to eliminate the audible noise, but that decreases η_e significantly. Besides, this method cannot be adopted for the *LLC* half-bridge converter, because f_s varies with the load variation and η_e decreases by the switching duty-control for V_o regulation.

This paper proposes a gate-pulse modulation, which decreases turn-on and turn-off losses by skipping several pairs of gate-control pulses under a light-load condition. This skip control increases η_e under both heavy- and light-load conditions. The concept and theoretical background of the proposed skip-control method are described in Section II, the design considerations are given in Section III, the control circuit and experimental results are given in Section IV, and a conclusion is given in Section V.

II. Skip Control of the *LLC* Resonant Half-Bridge Converter

Under light load, f_s of the LLC resonant half-bridge converter is higher than f_r [see Fig. 3(a)], so the switch turns OFF before the resonant current i_r decreases to zero. The remnant energy in L_r is transferred to C_r through the body diode of switch. This process increases power loss in the switch and in the resonant current path. The power loss under light load is reduced either when f_s can be kept close to f_r or when the power conversion is turned off periodically by turning off the gate pulses periodically. Under light load, the proposed skip-control method [see Fig. 3(b)] keeps f_s close to f_r by skipping several pairs of control pulses, so it can reduce both switching and conduction losses. The change of f_s required to regulate V_o is minimized because skip control varies Z_{eff} by using a gate-pulse modulation, so η_e under light load can be increased significantly. Also,

the skip control enables use of higher L_m than the normal control, and has less variation of f_s to regulate output voltage, so the use of large L_m reduces the current peak of magnetizing current and the resonance current, and thereby reduces the switching loss and the conduction loss of a transformer.

A. Voltage Conversion Ratio Under Skip Control

Without the skip control, bipolar square pulses of amplitude $V_{\rm in}/2$ are applied to the resonant circuit. The resonant circuit of the converter eliminates the higher harmonic current, so the fundamental harmonic approximation [22] can be used to calculate the voltage conversion ratio $V_o/V_{\rm in}$; the fundamental component of $V_{\rm in}$ is

$$\tilde{V}_{\rm in}(t) = \frac{2V_{\rm in}}{\pi}\sin(2\pi f_s t) \tag{1}$$

and the fundamental component of the rectifier input voltage is

$$\tilde{V}_{Lm}(t) = \frac{4V_o}{\pi}\sin(2\pi f_s t). \tag{2}$$

With the skip control, the fundamental component $V_{\rm in\_skip}(t)$ of input voltage can be represented as

$$V_{\rm in\_skip}(t) = \sum_{k=0}^{\infty}\tilde{V}_{\rm in}(t)\Big[u(t-k(N+1)T_s) - u(t-k(N+1)T_s - T_s)\Big] \tag{3}$$

where $T_s = 1/f_s$, $u(t)$ is the unit step function, and N is number of skipped pulse pairs. The Laplace transform of $V_{\rm in\_skip}(t)$ is

$$V_{\rm in\_skip}(s) = \left(\frac{2V_{\rm in}}{\pi}\frac{\omega_s}{s^2+{\omega_s}^2}\right)\left(\frac{1-e^{-sT_s}}{1-e^{-s(N+1)T_s}}\right) \tag{4}$$

where $\omega_s = 2\pi f_s$. When the input impedance of transformer is represented with an equivalent resistance $R_{\rm eq}$, the transfer function $H(s) \equiv V_{Lm}(s)/V_{\rm in\_skip}(s)$ is given by

$$H(s) = \frac{1}{1+(1+\omega_r^2/s^2)/K + \sqrt{L_r/C_r}(s/\omega_r + \omega_r/s)/R_{\rm eq}} \tag{5}$$

where $K \equiv L_m/L_r$ and $\omega_r = 2\pi f_r = 1/\sqrt{L_r C_r}$. An inverse Laplace transform of $V_{Lm}(s)$ results in the fundamental component of $V_{Lm}(t)$ as

$$\tilde{V}_{Lm}(t) = \frac{2V_{\rm in}}{\pi}|H(j\omega_s)|\sin(\omega_s t + \angle H(j\omega_s)) \times \sum_{k=0}^{\infty}[u(t-k(N+1)T_s) - u(t-k(N+1)T_s - T_s)]. \tag{6}$$

The average of the fundamental component of rectifier input is

$$\tilde{V}_{\rm rec,\,peak}(t) = \frac{4}{\pi}V_o \tag{7}$$

and the average of rectifier input current is

$$< \tilde{I}_{\rm rec}(t) > = \frac{2}{(N+1)T_s}\int_0^{T_S/2}\tilde{I}_{\rm rec,\,peak}\sin(\omega_s t)dt = \frac{2}{(N+1)\pi}\tilde{I}_{\rm rec,\,peak} = I_o \tag{8}$$

so the equivalent resistance of load at the rectifier input is

$$R'_{\rm eq} = \frac{\tilde{V}_{\rm rec,\,peak}}{\tilde{I}_{\rm rec,\,peak}} = \frac{8}{(N+1)\pi^2}R_L.$$

The $n:1$ transformer transforms $R'_{\rm eq}$ to

$$R_{\rm eq} = \frac{8n^2}{(N+1)\pi^2}R_L. \tag{9}$$

From (6), (7), and (9), the voltage conversion ratio M is calculated as

$$M = \frac{V_o}{V_{\rm in}} = \frac{\tilde{V}_{Lm,\rm peak}}{nV_{\rm in}} = \frac{1}{2n}\left(\left\{1+\frac{1}{K}\left(1-\frac{1}{{f_n}^2}\right)\right\}^2 + \left\{Q\left(f_n - \frac{1}{f_n}\right)\right\}^2\right)^{-1/2} \tag{10}$$

where $Q \equiv \pi^2(N+1)\sqrt{L_r/C_r}/(8n^2R_L)$ is an equivalent quality factor, and $f_n \equiv f_S/f_r$ is a normalized frequency. This equation shows that M can be adjusted by varying either f_s, K, N, or $R_L \equiv V_o/I_o$.

B. Determination of K and Q Under Full-Load Condition

The converter is assumed to operate at $f_{n,\min} = 0.4 \le f_n \le f_{n,\max} = 3.0$ to adjust M. The values of K and Q should be chosen to allow a gain variation $M_{\min} \le M \le M_{\max}$; $M_{\min}$ and $M_{\max}$ are calculated using (10) as

$$2nM_{\min} = \left(\left\{1+\frac{1}{K}\left(1-\frac{1}{{f_{n,\max}}^2}\right)\right\}^2 + \left\{Q\left(f_{n,\max} - \frac{1}{f_{n,\max}}\right)\right\}^2\right)^{-1/2} \tag{11}$$

$$2nM_{\max} = \left(\left\{1+\frac{1}{K}\left(1-\frac{1}{{f_{n,\min}}^2}\right)\right\}^2 + \left\{Q\left(f_{n,\min} - \frac{1}{f_{n,\min}}\right)\right\}^2\right)^{-1/2}. \tag{12}$$

The curves of $2nM_{\min}$ and $2nM_{\max}$ versus Q (see Fig. 4), were calculated at $f_{n,\max} = 3.0$ and $f_{n,\min} = 0.4$; $M_{\max}$ increased as either Q or K decreased, and $M_{\min}$ increased as either Q decreased or K increased. When it is desired to operate the converter at $M_{op,\min} \le M \le M_{op,\max}$ for a load variation 20–100%, $M_{\rm op,max} \le M_{\max}$ and $M_{\min} \le M_{\rm op,min}$ should be satisfied for $Q_{\min} \le Q \le Q_{\max}$. For a given $K, Q_{\max}$, which is the maximum value of Q at full load, is obtained using

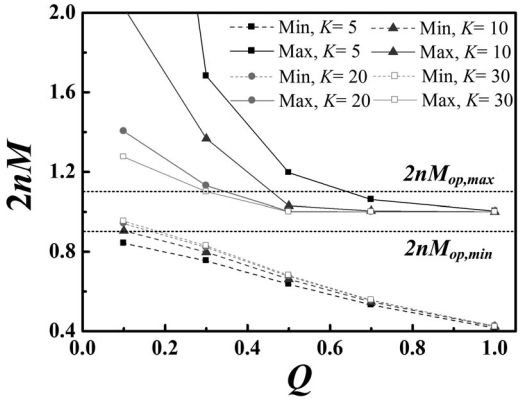

Fig. 4. Available gain $2nM$ versus Q for the *LLC* resonant half-bridge converter at $K = 5, 10, 20$, and 30, when the converter operates under the normal control.

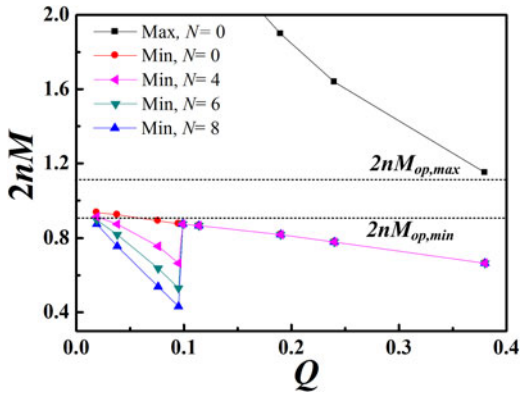

Fig. 5. Available gain $2nM$ versus Q for the *LLC* resonant half-bridge converter at $K = 8$; the converter operates under the skip control ($N = 0, 4, 6$, and 8) under a light-load ($Q \leq 0.095$) condition.

(12) as

$$Q_{\max} = \left| f_{n,\min} - \frac{1}{f_{n,\min}} \right|^{-1} \times \left(\frac{1}{{M_{op,\max}}^2} - \left\{ 1 + \frac{1}{K} \left(1 - \frac{1}{{f_{n,\min}}^2} \right) \right\}^2 \right)^{1/2} \tag{13}$$

after setting $M_{\max} = M_{\mathrm{op},\max}$. Because the converter uses the skip control to reduce M when the load is ≤20%, $Q_{\min} = 0.2Q_{\max}$ is calculated using (11) as

$$Q_{\min} = 0.2Q_{\max} = \left| f_{n,\max} - \frac{1}{f_{n,\max}} \right|^{-1} \times \left(\frac{1}{{M_{op,\min}}^2} - \left\{ 1 + \frac{1}{K} \left(1 - \frac{1}{{f_{n,\max}}^2} \right) \right\}^2 \right)^{1/2} \tag{14}$$

after setting $M_{\min} = M_{\mathrm{op},\min}$. K, which results $M_{\min} \leq M_{op,\min}$ at $Q = Q_{\min}$, is calculated using (11) as

$$K \leq \left(1 - \frac{1}{{f_{n,\max}}^2} \right) \left(\left[\left(\frac{1}{{M_{\mathrm{op},\min}}^2} - \left\{ Q_{\min} \left(f_{n,\max} - \frac{1}{f_{n,\max}} \right) \right\}^2 \right)^{1/2} - 1 \right] \right)^{-1}. \tag{15}$$

Because $Q_{\min} << 1$, this equation can be approximated as

$$K \leq \left(1 - \frac{1}{{f_{n,\max}}^2} \right) \left(\frac{1}{M_{\mathrm{op},\min}} - 1 \right)^{-1}. \tag{16}$$

C. Number of Skipped Periods N Under a Light-Load Condition

Under light load, the converter skips its control pulses to increase the power-conversion efficiency η_e and to widen the input voltage range. Because $Q = I_o(N+1)\pi^2\sqrt{L_r/C_r}/(8n^2V_o)$ when $N \neq 0$, Q at a light load can be adjusted by increasing N such that $Q \geq Q_{\max}$; this condition gives

$$N \geq \frac{I_{o,\max}}{I_o} - 1 \tag{17}$$

where $I_{o,\max}$ is the output current at full load. N should increase as I_o decreases. However, N can increase too much at a very light load, and cause an audible noise; the condition $f_s/(N+1) \geq 20$ kHz is required to prevent this problem. Therefore, using (17) and $f_s \approx f_r$, the range of N is

$$\frac{I_{o,\max}}{I_o} - 1 \leq N \leq 5 \times 10^{-5} f_r - 1. \tag{18}$$

Equations (13), (14), and (16) result in $K \leq 8$ and $0.05 \leq Q \leq 0.4$ for $2nM_{\mathrm{op},\max} = 1.1$, $2nM_{\mathrm{op},\min} = 0.9$, $f_{n,\min} = 0.4$, and $f_{n,\max} = 3.0$. Based on this, $K = 8$ and $Q = 0.38$ are chosen to examine the effectiveness of skip control. The $2nM$ versus Q curves for $N \neq 0$ (see Fig. 5) show that one can achieve $M_{\mathrm{op},\min} > M_{\min}$ even for $Q < 0.076$. So, the skip control enables us to use f_s close to f_r to adjust M of the converter under a light-load condition, that decreases the switching loss.

III. Design Considerations

A. Turns Ratio n of the Transformer

The converter was designed to operate at $V_o = 24$ V, 345 V $\leq V_{\mathrm{in}} \leq$ 425 V, and 7.2 W $\leq P_o \leq$ 360 W. To achieve high η_e over the range of V_{in}, the conditions $f_s = f_r$ at $V_{\mathrm{in,nom}} = (345 + 425)/2$ V = 385 V were desired. Because $M = 1/(2n)$ at $f_s = f_r$ from (10), the turns ratio n of the transformer was chosen as

$$n = \frac{345 + 425}{2V_o} \approx 8. \tag{19}$$

B. Resonance Frequency f_r

Under the normal control, the converter had $\eta_e \geq 94\%$ for $I_o/I_{o,\max} \geq 25\%$, but η_e for $I_o/I_{o,\max} < 20\%$ dropped quickly as $I_o/I_{o,\max}$ decreased. Therefore, the converter was operated under the skip control only when $I_o/I_{o,\max} \leq 25\%$. The skip

control adjusted the number N of skipped pulse pairs to regulate the gain under a light-load condition; it adjusts $2nM_{\mathrm{op,min}}$ for $Q < 0.1$ ($I_o/I_{o,\max} < 25\%$) in Fig. 5. The largest $N, N_{\max}$ should be smaller than $f_s/(20\,\mathrm{kHz}) - 1$ to avoid an audible noise generation; $N_{\max}$ should be the smallest number that satisfies $2nM_{\mathrm{op,min}} \leq 0.9$ at the lightest load. In the case that $I_o/I_{o,\max} = 5\%$ ($Q = 0.019$) was the lightest load, $N_{\max} = 8$ resulted in $2nM_{op,\min} < 0.9$ for $5\% \leq I_o/I_{o,\max} \leq 100\%$ (see Fig. 5). Then, the lowest resonance frequency $f_{r,\min}$ should be higher than $(N_{\max} + 1)$ 20 kHz = 180 kHz to have $f_s > f_r$ for $2nM < 1$. When $I_o/I_{o,\max} < 5\%$, the converter increased f_s to regulate V_o, instead of increasing N.

C. Resonant Components L_r and C_r

The following equations were obtained using $Q = \sqrt{L_r/C_r}/R_{\mathrm{eq}}$ and $f_r = 1/(2\pi\sqrt{L_rC_r})$:

$$L_r = \frac{QR_{\mathrm{eq}}}{2\pi f_r} \tag{20}$$

$$C_r = \frac{1}{2\pi f_r QR_{\mathrm{eq}}}. \tag{21}$$

$R_{\mathrm{eq}} = (8n^2/\pi^2)(V_o/I_{o,\max}) = 83.08\ \Omega$ for $n = 8, Q = 0.38$, $f_r = 180\,\mathrm{kHz}$, $V_o = 24\,\mathrm{V}$, and $I_{o,\max} = 15\,\mathrm{A}$ ($P_o = 360\,\mathrm{W}$), so $L_r = 30\,\mu\mathrm{H}$ and $C_r = 26\,\mathrm{nF}$.

D. Magnetizing Inductance L_m

To have a zero-voltage turn-on of SW_1 and SW_2, the output capacitances $C_{\mathrm{DS1}} = C_{\mathrm{DS2}} = C_{\mathrm{DS}}$ of SW_1 and SW_2 should be completely charged or discharged by the magnetizing current I_{Lm} during the dead time t_d. Because $f_s = f_r f_{n,\max}$ at $V_{\mathrm{in},\max}$ and $I_{Lm} \approx nV_o/(4L_m f_s)$ during t_d, this condition requires $I_{Lm}t_d \geq 2C_{\mathrm{DS}}V_{\mathrm{in}}$, so

$$L_m \leq \frac{nV_o t_d}{8C_{\mathrm{DS}}V_{\mathrm{in},\max}f_r f_{n,\max}}. \tag{22}$$

The converter is required to have $K = L_m/L_r = 8$ (see Section II-C); as a result, $L_m = KL_r = 240\ \mu\mathrm{H}$ for $L_r = 30\ \mu\mathrm{H}$. When the converter was implemented using the circuit parameters of $C_{\mathrm{DS}} = 59$ pF, $f_{n,\max} = 3f_r = 540$ kHz, and $nV_o/V_{\mathrm{in},\max} = 0.9/2 = 0.45$, the condition (22) resulted in $t_d \geq 135$ ns; the converter was operated at $t_d = 160$ ns, considering $t_d \geq 135$ ns and that the MOSFET switches (SPA17N80CS, Infineon) require a minimum switching delay > 131 ns.

IV. Experimental Results

The *LLC* resonant converter (see Fig. 6) was designed to operate $345 \leq V_{\mathrm{in}} \leq 425$ V at $V_o = 24$ V, $f_r = 180$ kHz, and $7.2\,\mathrm{W} \leq P_o \leq 360\,\mathrm{W}$ ($0.3\,\mathrm{A} \leq I_o \leq 15\,\mathrm{A}$); it was implemented using the following circuit parameters: $n = 8, L_m = 240\,\mu\mathrm{H}, L_r = 30\,\mu\mathrm{H}$, and $C_r = 26\,\mathrm{nF}$ (see Section III). This converter was operated using the proposed skip-control method (skip control), the burst-control method presented in [19] (burst control), or the control method presented in [20]. The converter was also operated using the normal-control method [23] after changing L_m to 120 μH to secure the input voltage range

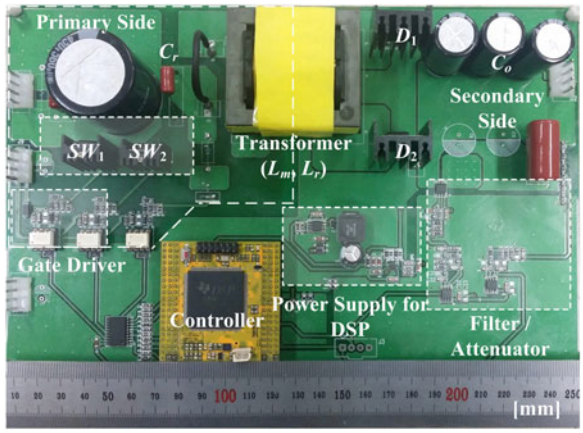

Fig. 6. Photograph of the experimental *LLC* resonant half-bridge converter.

(normal control), and using the burst-control method after changing C_r to 6.8 nF to have $f_r = 350$ kHz (high-f_r burst control) that eliminated audible noise generation.

The circuit for skip control (see Fig. 7) was implemented using a dc power supply, a filter/attenuator circuit, and a digital signal processor (DSP, TMS320F28335, Texas instruments). The dc power supply steps down V_{in} to 5 V for DSP, and the filter/attenuator circuit filters/attenuates V_o and I_o to a voltage range of 0–3 V.

The DSP consists of a compensator, a mode selector, a pulse width modulation (PWM) generator, an analog-to-digital converter (ADC), and a protection circuit. The ADC converts V_o and I_o to digital signals $V_{o,\mathrm{sen}}[n]$ and $I_{o,\mathrm{sen}}[n]$, where n is the sampling number. The compensator calculates the difference $e[n]$ between $V_{o,\mathrm{sen}}[n]$ and a reference voltage V_{o_ref}, and generates an output signal $T_b[n] = K_P e[n] + K_I \sum_{i=0}^{n} e[i]$, where K_P is the proportional gain and K_I is the integration gain. The switching period $T_s[n]$ is corrected as $T_s[n] = T_s[n-1] + T_b[n]$, where $T_s[n-1]$ is the previous sampling number; $T_s[0] = 1/f_{\max}$ has been used to prevent a sudden change of V_o. The 16-b counter counts the 75 MHz CLK until the counter output $T_c[m]$ reaches $T_s[n]$. A PWM signal D is generated using $T_c[m]$ such that $D = 1$ for $T_c[m] < T_s[n]/2$ and $D = 0$ for $T_c[m] \geq T_s[n]/2$. Then, two of PWM signals that have a switching duty of 50% and a phase difference of 180° are generated.

The mode selector uses $I_{o,\mathrm{sen}}[n]$ and full-load current $I_{o,\max}$, checks the condition $I_{o,\mathrm{sen}}[n] \leq 0.2I_{o,\max}$, and calculates the number $N[n] = \mathrm{Interger}(I_{o,\max}/I_{o,\mathrm{sen}}[n]) - 1$ of pulses being skipped if $I_{o,\mathrm{sen}}[n] \leq 0.2I_{o,\max}$. The selector also counts the number $C[i]$ of reset pulses for the 16-b counter: $C[i] = 1$ if $N[n] = 0$, or $C[i]$ is reset to 0 either when $C[i] = N[n] + 1$ or when $C[i] = 9$. Then, the mode selector outputs the control pulses R for the Flip/Flops: $R = 0$ if $C[i] = 1, R = 1$, otherwise.

The waveforms of V_o, I_r, V_{G1}, and V_{G2} (see Fig. 8) were measured at $V_{in} = 385$ V and $V_o = 24$ V, while stepping down I_o abruptly from 5 to 1 A. These waveforms show the following: V_o changed little and I_r adjusted smoothly for the given change of I_o [see Fig. 8(a)], and the converter operated in the nonskip

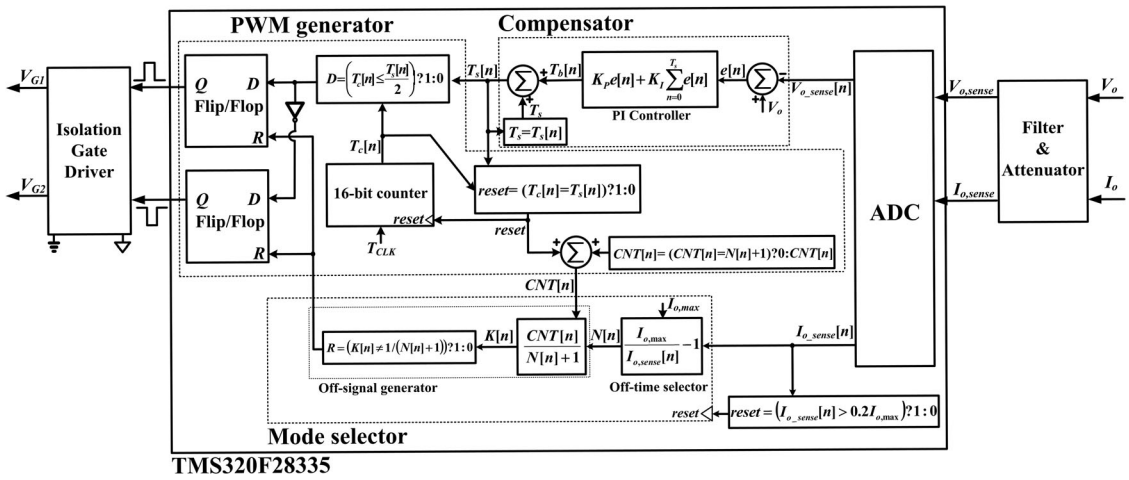

Fig. 7. Block diagram of control circuit for the skip control.

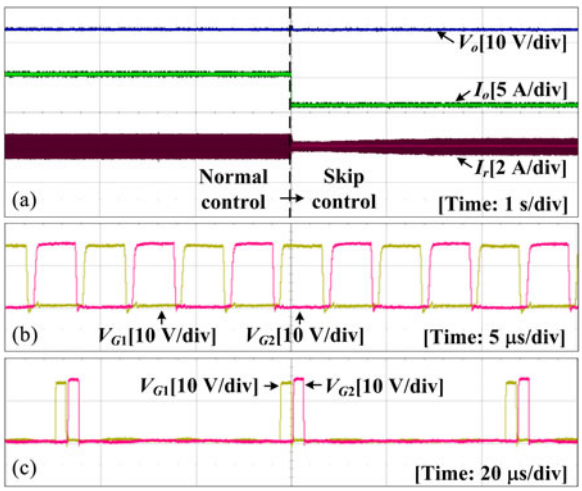

Fig. 8. Experimental waveforms of the converter; measured at $V_{\rm in} = 385$ V and $V_o = 24$ V, while stepping down I_o abruptly from 5 to 1 A; (a) V_o, I_o, and I_r, (b) V_{G1} and V_{G2} at $I_o = 5$ A, and (c) V_{G1} and V_{G2} at $I_o = 1$ A.

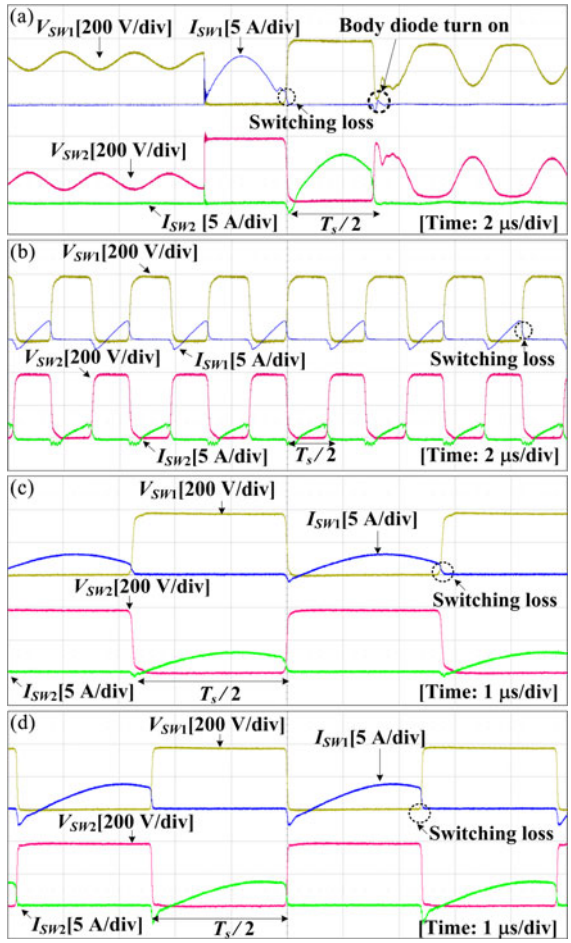

Fig. 9. Voltage and current waveforms of switches at $V_{\rm in} = 385$ V and $V_o = 24$ V; measured while operating the converter using (a) the skip control at $I_o = 2$ A, (b) the normal control at $I_o = 2$ A, (c) the skip control at $I_o = 15$ A, and (d) the normal control $I_o = 15$ A.

control mode at $I_o = 5$ A and in the skip control mode at $I_o = 1$ A [see Fig. 8(b) and (c)].

The voltage and current waveforms of $\rm SW_1$ and $\rm SW_2$ (see Fig. 9) were measured at $V_{\rm in} = 385$ V, $V_o = 24$ V, and $I_o = 2$ A and 15 A. The converter was operated in the skip mode at $I_o = 2$ A [see Fig. 9(a)] and, therefore, at a lower f_s and had less switching loss than the normal control did [see Fig. 9(b)]. The skip control produced a parasitic resonance between $L_m + L_r$ and the source–drain capacitances of switches when both $\rm SW_1$ and $\rm SW_2$ were turned OFF, which was observed [see Fig. 9(a)] as voltage oscillations in V_{SW1} and V_{SW2}. However, this parasitic oscillation had little influence on η_e because some energy stored in L_r and L_m was recovered by $C_{\rm IN}$ and C_r; the parasitic oscillation did not increase the voltage stress of switches because the oscillation voltage was less than $V_{\rm in}$, and influenced little the temperature-related circuit reliability because the oscillation current was very low. At $I_o = 15$ A, the converter was operated in a nonskip mode [see Fig. 9(c)]. Compared to the waveforms for the normal control using $L_m = 120$ μH [see Fig. 9(d)], the skip control enabled $L_m = 240$ μH, so I_{SW1} and I_{SW2} were decreased and the switching loss was reduced.

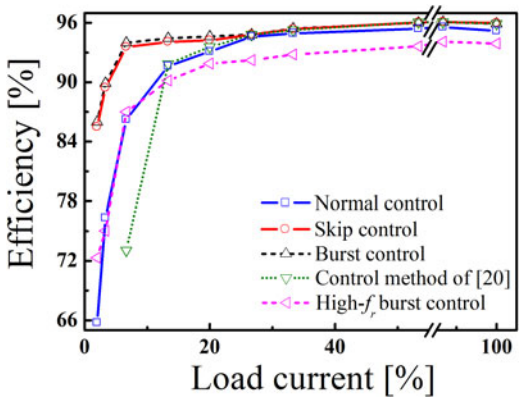

Fig. 10. η_e versus $I_o/I_{o,\max}$ for the converter using the normal, skip, burst, and high-f_r burst controls, and using the control method presented in [20]; measured at $V_{\rm in} = 385$ V, $V_o = 24$ V, and $2\% \le I_o/I_{o,\max} \le 100\%$.

The η_e versus $I_o/I_{o,\max}$ curves of the *LLC* resonant converters (see Fig. 10) were measured at $V_{\rm in} = 385$ V, $V_o = 24$ V, 0.3 A $(I_o/I_{o,\max} = 2\%) \le I_o \le 15$ A $(I_o/I_{o,\max} = 100\%)$. All controls resulted in $\eta_e = 95.98\%$ at $I_o = 15$ A (100%), except for the normal and high-f_r burst controls, which resulted in $\eta_e = 95.18\%$ and 93.91%, respectively; $L_m = 120$ μH for the normal control was one half of $L_m = 240$ μH for the other controls; that reduction increased the magnetizing current I_{Lm}, so the transformer loss was increased. The high-f_r burst control resulted in the lowest η_e for $I_o \ge 2$ A $(I_o/I_{o,\max} \ge 13.3\%)$ because f_r was increased to 350 kHz.

η_es at $I_o = 0.3$ A $(I_o/I_{o,\max} = 2\%)$ were 65.74% (normal control), 85.46% (skip control), 85.98% (burst control), and 72.32% (high-f_r burst control); the converter using the control method presented in [20] failed at this measurement condition because this method resulted in unstable operation of the converter when $D < 0.1$ $(I_o/I_{o,\max} < 6.6\%)$. η_e of the normal control decreased rapidly as I_o decreased, because f_s increased significantly from f_r, and thereby increased the switching loss. Also, η_e of the control methodin [20] decreased rapidly as I_o decreased; in this case, $f_s = f_r$ and D decreased as I_o decreased, so the switch current was higher than that of the other controls. η_e of the burst control was 0.52% higher than that of the skip control, because the burst control produced hard switching only at the beginning of pulse train, whereas the skip control produced hard switching at every first pulse. However, the skip control eliminated audible noise and reduced output ripple voltage. η_e of the high-f_r burst control was 13.14% lower than that of the skip control, because it used $f_r = 350$ kHz to eliminate audible noise.

The power losses in the *LLC* resonant converters were analyzed at $V_{\rm IN} = 385$ V, $V_O = 24$ V, and $I_o = 1$ A using a circuit simulator (see Table I). The total power losses were 3.905 W (normal control), 1.648 W (skip control), 1.604 W (burst control), and 3.473 W (high-f_r burst control); the losses in rectifying diodes D_1 and D_2 were reduced significantly under the skip and burst controls, because f_s was close to f_r. The high-f_r burst control required the highest f_s, which increased the power losses in switches and diodes.

TABLE I
POWER LOSSES IN THE *LLC* RESONANT CONVERTER UNDER DIFFERENT CONTROLS

Component	Power Loss (%)			
	Normal	Skip	Burst	High-f_r Burst
SW_1	9.09	5.762	5.736	7.706
SW_2	8.732	5.744	5.744	7.289
D_1	34.16	29.17	28.93	35.05
D_2	33.93	28.81	28.55	35.59
$L_m + L_r$	13.85	29.96	30.67	14.11
C_r	0.23	0.546	0.561	0.259
Total loss (W)	3.905	1.648	1.604	3.473

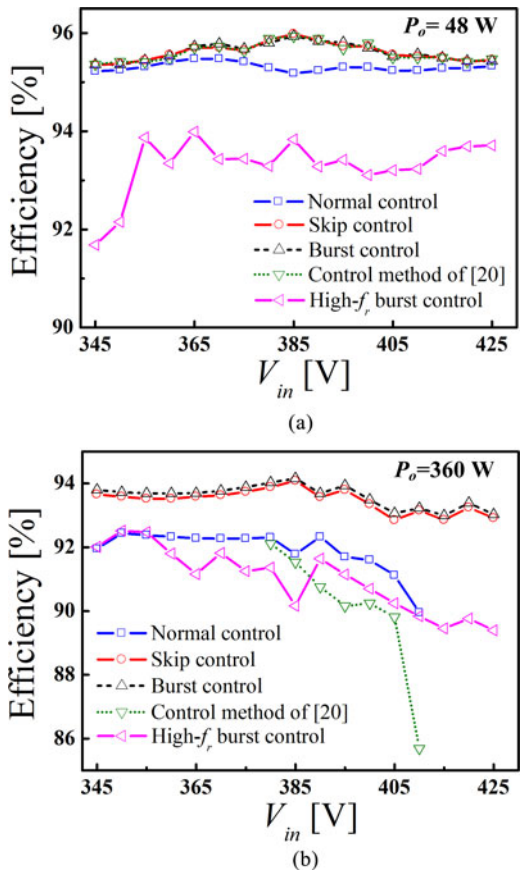

Fig. 11. η_e versus $V_{\rm in}$ for the converter using the normal, skip, burst, and high-f_r burst controls, and using the control method presented in [20]; measured at (a) $V_{\rm o} = 24$ V and $I_{\rm o} = 15$ A, and (b) $V_{\rm o} = 24$ V and $I_{\rm o} = 2$ A.

The η_e versus $V_{\rm in}$ curves were measured at $I_o = 15$ A [100%, Fig. 11(a)] and at $I_o = 2$ A [13.3%, Fig. 11(b)]. All controls were operated properly at $345 \le V_{\rm in} \le 425$ V; the converters were operated differently only under light load. At $I_o = 15$ A, the curves for the skip and burst controls and for the control method presented in [20] were almost identical $(95.35\% \le \eta_e \le 95.98\%)$; at any $V_{\rm in}$, the normal control had slightly lower η_e $(95.17\% \le \eta_e \le 95.47\%)$ than these three controls because the normal control required lower L_m than the others to widen the input voltage and output power ranges. The high-f_r burst

TABLE II
OUTPUT RIPPLE VOLTAGES AT DIFFERENT LOAD CONDITIONS; THE EXPERIMENTAL CONVERTER WAS OPERATED USING THE BURST AND PROPOSED CONTROLS

Load (%)	ΔV_o (mV)	
	Burst	Skip
3.3	51	10
6.6	97	17
13.3	158	20
20	150	23

TABLE III
LOWEST COMPONENT OF SWITCHING FREQUENCY AT DIFFERENT LOAD CONDITIONS

Load (%)	$f_{s,\text{lowest}}$ (kHz)	
	Burst	Skip
3.3	2.18	20.7
6.6	2.71	21.2
13.3	3.12	25.4
20	3.91	35.3

control had the lowest η_e $(91.68\% \leq \eta_e \leq 93.83\%)$ over the whole range of input voltage.

At $I_o = 2$ A, different controls resulted in different η_es and input voltage ranges: $89.94\% \leq \eta_e \leq 92.43\%$ and 345 V $\leq V_{\text{in}} \leq$ 410 V for the normal control, $85.69\% \leq \eta_e \leq 92.11\%$ and $380 \leq V_{\text{in}} \leq 410$ V for the control method of [20], $92.99\% \leq \eta_e \leq 94.15\%$ and $345 \leq V_{\text{in}} \leq 425$ V for the burst control, $92.91\% \leq \eta_e \leq 94.08\%$ and $345 \leq V_{\text{in}} \leq 425$ V for the skip control, and $89.39\% \leq \eta_e \leq 92.01\%$ and $345 \leq V_{\text{in}} \leq 425$ V for the high-f_r burst control. The normal control could not have $V_{\text{in}} > 410$ V because it required $f_s > f_{s,\max} = 540$ kHz to decrease the voltage gain. The control method proposed in [20] decreased η_e as V_{in} increased, because D decreased as V_{in} increased, instead of varying f_s. The high-f_r burst control decreased η_e as V_{in} increased, because f_s increased as V_{in} increased. The burst and skip controls had the highest η_e and the widest input voltage range, because they varied both f_s and N to vary the voltage gain.

When the output ripple voltage ΔV_o and the lowest component of switching frequency $f_{s,\text{lowest}}$ were measured at $V_{\text{in}} = 385$ V and $V_o = 24$ V (see Tables II and III), the skip control had $\Delta V_o = 23$ mV [see Fig. 12(a)] and $f_{s,\text{lowest}} = 35.3$ kHz at $I_o = 3$ A $(I_o/I_{o,\max} = 20\%)$, whereas the burst control had $\Delta V_o = 150$ mV and $f_{s,\text{lowest}} = 3.91$ kHz [see Fig. 12(b)]. The skip control had $f_{s,\text{lowest}} = 21.2$ kHz even at $I_o = 1$ A $(I_o/I_{o,\max} = 6.6\%)$. These results (Fig. 11; Tables II and III) show that the skip control can be used in applications that require no audible noise, wide input voltage range, and wide load variation.

The step-load responses of V_o for the converter that uses skip control (see Fig. 13) were measured at $V_{\text{in}} = 385$ V, $V_o = 24$ V while changing I_o from 5 (normal control) to 2 A (skip control) abruptly, and from 2 to 5 A. When I_o stepped down from 5 to 2 A, V_o varied by < 1 V, and returned to a steady state after 70 ms [see Fig. 13(a)]. When I_o stepped up from 2 to 5 A, V_o also varied < 1 V, and returned to a steady state after 50 ms [see Fig. 13(b)]. These results show that skip control can be applicable for the systems that undergo a sudden change of load.

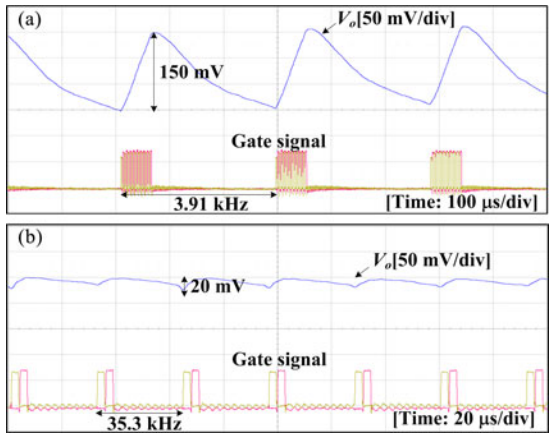

Fig. 12. Waveforms of V_o and gate pulses for $V_{\text{in}} = 385$ V, $V_o = 24$ V, and $I_o = 3$ A: (a) burst and (b) skip controls. Nine pair of burst control pulses resulted in $\Delta V_o = 150$ mV at $I_o = 3$ A.

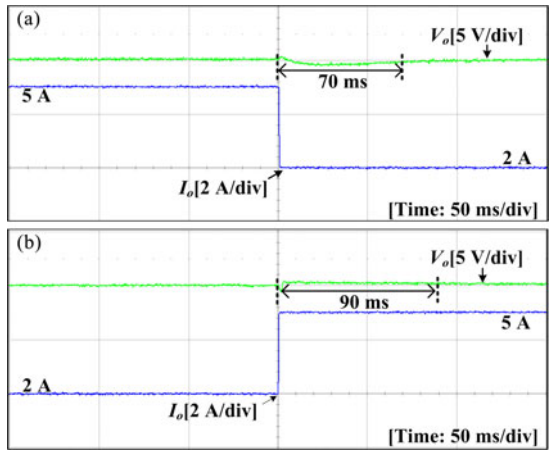

Fig. 13. Step-load responses of V_o for the converter using the skip control; measured at $V_{\text{in}} = 385$ V and $V_o = 24$ V, while changing I_o (a) from 5 to 2 A, and (b) from 2 to 5 A.

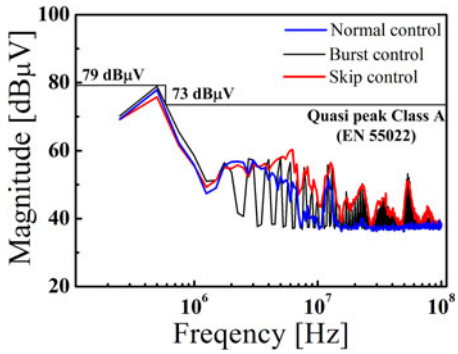

Fig. 14. Noise spectrum of I_{in} measured at $V_{\text{in}} = 385$ V, $V_o = 24$ V, and $I_o = 2$ A, while operating the converter using the normal, skip, and burst controls.

The noise spectrum (see Fig. 14) of input current $I_{\rm in}$ was measured at $V_{\rm in} = 385\,{\rm V}$, $V_o = 24\,{\rm V}$, and $I_o = 2$ A using a spectrum analyzer (E4480B, Agilent Inc.). The skip control increased the noise in the frequency range of 3–100 MHz, but satisfied the EN 55022 class A specifications that are the industry standard for electronic devices.

V. Conclusion

The proposed skip-control method reduced switching and conduction losses under light load by skipping several pairs of switch-control pulses, while varying the switching frequency less than the normal-control method does. This method allowed us to use a large magnetizing inductance for the *LLC* resonant converter, and had high η_e over a wide range of loads. It also allowed wider input and output ranges than the normal-control method does. The skip-control method could prevent audible noise generation in an *LLC* resonant half-bridge dc–dc converter under a light-load condition, while achieving the same η_e as the burst-control method. These results show that the proposed method is useful for applications that require no audible noise, wide input voltage range, and wide load variation.

References

[1] B. C. Kim, K. B. Park, C. E. Kim, B. H. Lee, and G. W. Moon, "LLC resonant converter with adaptive link-voltage variation for a high-power-density adapter," *IEEE Trans. Power Electron.*, vol. 25, no. 9, pp. 2248–2252, Sep. 2010.

[2] R. Beiranvand, B. Rashidian, M. R. Zolghadri, and S. M. H. Alavi, "Using LLC resonant converter for designing wide-range voltage source," *IEEE Trans. Ind. Electron.*, vol. 58, no. 5, pp. 1746–1756, May 2011.

[3] S. H. Cho, C. W. Roh, S. S. Hong, and S. K. Han, "High-efficiency and low-cost tightly-regulated dual-output LLC resonant converter," in *Proc. IEEE Int. Symp. Ind. Electron.*, Jul. 2010 pp. 862–869.

[4] W. Feng, F. C. Lee, P. Mattavelli, and D. Huang, "A universal adaptive driving scheme for synchronous rectification in LLC resonant converters," *IEEE Trans. Power Electron.*, vol. 27, no. 8, pp. 3775–3781, Aug. 2012.

[5] X. Fang *et al.*, "Efficiency-oriented optimal design of the LLC resonant converter based on peak gain placement," *IEEE Trans. Power Electron.*, vol. 28, no. 5, pp. 2285–2296, May 2013.

[6] S. Y. Chen, Z. R. Li, and C. L. Chen, "Analysis and design of single-stage AC/DC LLC resonant converter," *IEEE Trans. Ind. Electron.*, vol. 59, no. 3, pp. 1538–1544, Mar. 2012.

[7] F. C. Lee, S. Wang, P. Kong, C. Wang, and D. Fu, "Power architecture design with improved system efficiency, EMI and power density," in *Proc. IEEE Power Electron. Spec. Conf.*, Jun. 2008, pp. 4131–4137.

[8] B. Lu, W. Liu, Y. Liang, F. C. Lee, and J. D. Van Wyk, "Optimal design methodology for LLC resonant converter," in *Proc. IEEE. Appl. Power Electron. Conf. Expo.*, Mar. 2006 pp. 533–538.

[9] J. H. Kim, C. E. Kim, J. K. Kim, and G. W. Moon, "Analysis for LLC resonant converter considering parasitic components at very light load condition," in *Proc. IEEE ECCE Asia*, Jun. 2011 pp. 1863–1868.

[10] B. Yang, F. C. Lee, A. J. Zhang, and G. Huang, "LLC resonant converter for front end DC/DC conversion," in *Proc. IEEE Appl. Power Electron. Conf. Expo.*, Mar. 2002, pp. 1108–1112.

[11] O. Trescases and W. Yue, "A survey of light-load efficiency improvement techniques for low-power DC-DC converters," in *Proc. IEEE 8th Int. Conf. Power Electron. ECCE Asia*, May/Jun. 2011 pp. 326–333.

[12] W. Yu, J. S. Lai, W. H. Lai, and H. Wan, "Hybrid resonant and PWM converter with high efficiency and full soft-switching range," *IEEE Trans. Ind. Electron.*, vol. 27, no. 2, pp. 4925–4932, Dec. 2012.

[13] A. A. Fomani and W. T. Ng, "A segmented gate driver with adjustable driving capability for efficiency optimization," in *Proc. Energy Convers. Congr. Expo*., Sep. 2010 pp. 2430–2433.

[14] Y. Jang and M. M. Jovanovic, "Light-load efficiency optimization method," *IEEE Trans. Power Electron.*, vol. 25, no. 1, pp. 67–74, Jan. 2010.

[15] L. Huber and M. M. Jovanovic, "Methods of reducing audible noise caused by magnetic components in variable-frequency-controlled switch-mode converters," *IEEE Trans. Power Electron.*, vol. 26, no. 6, pp. 1673–1681, Jun. 2011.

[16] B. Wang, X. Xin, S. Wu, H. Wu, and J. Ying, "Analysis and implementation of LLC burst mode for light load efficiency improvement," in *Proc. 24th Annu. IEEE Appl. Power Electron. Conf. Expo.*, Feb. 2009 pp. 58–64.

[17] Z. Hu, Y. Qiu, L. Wang, and Y. F. Liu, "An interleaved LLC resonant converter operating at constant switching frequency," *IEEE Trans. Power Electron.*, vol. 29, no. 6, pp. 2931–2943, Jun. 2014.

[18] W. J. Lee, S. W. Choi, C. E. Kim, and G. W. Moon, "A new PWM-controlled quasi-resonant converter for a high efficiency PDP sustaining power module," *IEEE Trans. Power Electron.*, vol. 23, no. 4, pp. 1782–1790, Jul. 2008.

[19] Y. C. Chen, T. J. Liang, W. J. Tseng, J. Y. Lee, and L. S. Yang, "Design and implementation of LLC resonant converter with high efficiency at light load condition," in *Proc. IEEE Power Electron. Distrib. Gener. Syst.*, Jun. 2010 pp. 538–542.

[20] H. Pan, C. He, F. Ajmal, H. Chen, and G. Chen, "Pulse-width modulation control strategy for high efficiency LLC resonant converter with light load applications," *IET Trans. Power Electron.*, vol. 7, no. 11, pp. 2887–2894, Oct. 2014.

[21] B. C. Mandi, S. Kapat, and A. Patra, "Fractional pulse skipping in digitally controlled DC-DC converters for improved light-load efficiency and power spectrum," in *Proc. IEEE Appl. Power Electron. Conf. Expo.*, May 2016 pp. 2504–2510.

[22] R. L. Steigerwald, "A comparison of half-bridge resonant converter topologies," *IEEE Trans. Power Electron.*, vol. 3, no. 2, pp. 174–182, Apr. 1988.

[23] K. Jin and X. Ruan, "Hybrid full-bridge three-level LLC resonant converter—A novel DC–DC converter suitable for fuel-cell power system," *IEEE Trans. Ind. Electron.*, vol. 53, no. 5, pp. 1492–1503, Oct. 2006.

Ho-Young Yoon received the B.S. degree in electronics engineering from Hanyang University, Ansan, South Korea, in 2012, and the M.S. degree in electrical engineering in 2014 from the Pohang University of Science and Technology, Pohang, South Korea, where he is currently working toward the Ph.D. degree in electrical engineering.

His research interests include the OLED driving circuit, digital control circuit, and soft-switching techniques in dc–dc converters.

Hyeon-Seok Lee received the B.S. degree in electrical engineering from Chungnam National University, Daejeon, South Korea, in 2013, and the M.S. degree in electrical engineering from the Pohang University of Science and Technology, Pohang, South Korea, in 2015, where he is currently working toward the Ph.D. degree in electrical engineering.

His research interests include the LED driving circuit, soft-switching techniques in dc–dc converters, and microinverters.

Seok-Hyeong Ham received the B.S. degree in electrical engineering from Pusan National University, Busan, South Korea, in 2013, and the M.S. degree in electrical engineering from the Pohang University of Science and Technology, Pohang, South Korea, in 2015, where he is currently working toward the Ph.D. degree in electrical engineering.

His research interests include the LED driving circuit, power-factor-correction circuits, and microinverter.

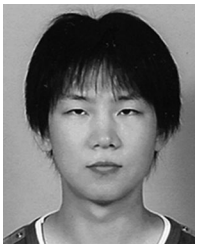

Hyung-Jin Choe received the B.S. degree in electrical engineering from Chungnam National University, Daejeon, South Korea, in 2009, and the M.S. and Ph.D. degrees in electrical engineering from the Pohang University of Science and Technology, Pohang, South Korea, in 2011 and 2014, respectively.

He is currently an Engineer with LG Display Co., Ltd., Paju, South Korea. His research interests include the power-factor-correction circuits, new converter topologies, and soft-switching techniques in ac–dc and dc–dc converters.

Bongkoo Kang (S'83–M'86) received the Ph.D. degree in electrical engineering from the University of California Berkeley, Berkeley, CA, USA, in 1986.

Following his graduation, he joined the Electronics and Telecommunication Research Laboratory, Daejeon, South Korea, where he worked on developing semiconductor processing equipment. Since 1989, he has been a Professor with the Department of Electrical Engineering, Pohang University of Science and Technology, Pohang, South Korea. His current research interests include the design of drive circuits for display devices and the modeling and characterization of semiconductor devices.